y metadata, citation and similar papers at core.ac.uk

brought to you by CO

provided by

Journal of Composite Materials
0(0) 1–11
© The Author(s) 2014
Reprints and permissions:
sagepub.co.uk/journalsPermissions.nav
DOI: 10.1177/0021998313519282
jcm.sagepub.com
SAGE

Damage in flax/epoxy quasi-unidirectional woven laminates under quasi-static tension

Malika Kersani[1,2], Stepan V Lomov[2], Aart Willem Van Vuure[2], Ahcène Bouabdallah[1] and Ignaas Verpoest[2]

Abstract

The damage initiation and development in flax/epoxy laminates under quasi-static tension is studied. The laminates are made of quasi-unidirectional woven prepregs in different configurations $[0^\circ]_8$, $[0^\circ, 90^\circ]_{2S}$, $[-45^\circ, 45^\circ]_{2S}$ and $[0^\circ, 90^\circ, +45^\circ, -45^\circ]_S$, and processed using an autoclave. The damage was monitored during the tensile test using acoustic emission and observed by post-mortem microscopy of the samples. The stress–strain curves illustrate the ductile behaviour of the $[+45^\circ, -45^\circ]_{2S}$ composite, whereas in the other composites a more brittle behaviour was observed. Non-linearity of the stress–strain curves is explained by the intrinsic non-linearity of flax fibres in tension. The combination of the stress–strain data and the registered acoustic emission data is used to identify the damage initiation and propagation thresholds. The damage thresholds are the lowest in the $[0^\circ]_8$ laminate and the highest in the $[+45^\circ, -45^\circ]_{2S}$ laminate. The observed fracture zones and damage mode are cracks inside and on the boundary of technical fibres, cracks on the boundary of tows, matrix cracking, fibre pull-out and fibre breakage. A notable feature of the damage behaviour is almost full absence of transverse matrix cracks inside tows in 90° plies, which are the major damage modes in glass- and carbon-reinforced plastics. This is attributed to the low stress concentrations in transverse direction due to the low transverse modulus of flax fibres.

Keywords

Flax fibre composites, damage, acoustic emission, mechanical properties

Introduction

In recent years, composites reinforced with natural fibres have attracted the curiosity of many researchers. Because of numerous advantages of natural fibres, such as good specific mechanical properties, renewability of raw material, low density (50–60% of the E-glass density), non-abrasive behaviour, safer handling, low cost and excellent potential to reduce carbon dioxide emissions, natural fibres are promising candidates for composite reinforcement. Even with drawbacks inherently present in natural cellulose-based fibres, such as their hydrophilic nature, wider properties variation, difficult adhesion to thermoset and especially thermoplastic resins, economical factors, etc., natural fibres are being extensively explored by automotive, aviation, marine, civil and packaging industries as an environment-friendly alternative to synthetic fibre composites.[1] Flax is probably the most commonly used bast-type fibre today. Due to its properties and availability, flax fibres have the potential to substitute glass fibres in polymer composites, even though their strength is lower.

Flax fibres can be classified into elementary fibres (sometimes referred to as 'fibre ultimates'[2]), which are grouped into so-called technical fibres consisting of 2–5 elementary fibres, as it is illustrated in Figure 1. The elementary fibres are kept together mainly by pectins, meaning that the technical fibres themselves are

[1]Faculty of Physics, University of Science and Technology Houari Boumediene, Algiers, Algeria
[2]Department of Metallurgy and Materials Engineering, KU Leuven, Leuven, Belgium

Corresponding author:
Stepan V Lomov, Department of Metallurgy and Materials Engineering, Katholic University, Kasteelpark Arenberg 44, Leuven 3001, Belgium.
Email: stepan.lomov@mtm.kuleuven.be

Downloaded from jcm.sagepub.com at KU Leuven University Library on March 13, 2015

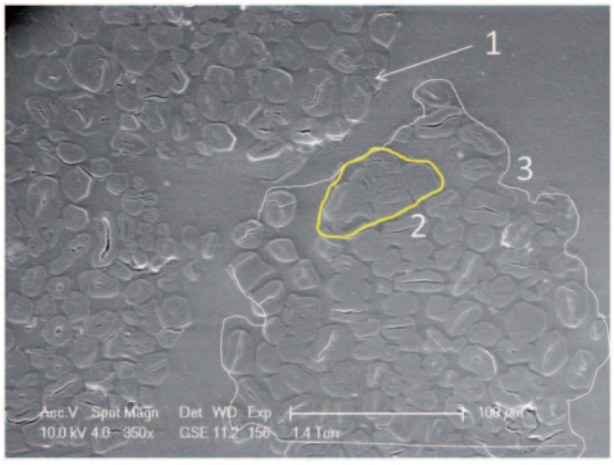

Figure 1. Fibrous structure of flax prepreg: 1, elementary fibre; 2, technical fibre; 3, yarn.

actually composite structures. Technical fibres have a diameter of 30–300 µm, whereas elementary fibres have a diameter of 15–35 µm.[3] The elementary fibres are the single plant cells consisting of concentric cell walls. Morphologically, an elementary fibre consists of a primary thin cell wall, a secondary thick cell wall and a lumen (of variable dimensions) – an open channel in the centre of the fibre. Primary and secondary cell walls differ in composition as well as in thickness. The primary cell wall which forms ~10% of the fibre's diameter consists mainly of cellulose microfibrils embedded in a matrix of pectin, hemicelluloses and small quantities of lignin.[4,5] The secondary cell wall constitutes the bulk part of the cell cross section, it consists of cellulose microfibrils bounded with pectin and hemicellulose. The numerous helically wound cellular microfibrils are often laid down in layers having defined orientations (microfibrillar angle) with the axis of the fibre.[6] A difference in physical, chemical and mechanical properties results from these morphological and constitutional differences between the two walls. The elementary flax fibre contains 65–75% of crystalline cellulose, ~15% of amorphous hemicellulose and 10–15% of pectin.[5]

Prior studies[7] determined the mechanical properties of a single flax fibre. It has been shown that the tensile strain–stress curves exhibit a non-linear behaviour at the early stage of loading, with the fibre stiffness decreasing when the applied strain reaches 0.1...0.3%, followed by the stiffness increase till 1.5% strain and linear stress–strain curve after. This complex behaviour is explained in ref. [7] to be a result of change of orientation of the structural components of the fibre cell wall (cellulosic microfibrils): relative movement of the microfibrils in the amorphous 'matrix', which defines the initial softening, and subsequent alignment of the microfibrils with the fibre axis, which leads to final stiffening. The initial softening can also be a result of 'kink bands' type of resistance.[6] The specific non-linearity of the stress–strain curve is an intrinsic characteristic of flax fibre (similar fibres, such as hemp or ramie, exhibit the similar behaviour), which will manifest itself in the yarn and composite tensile response. Flax mechanical properties show a large scattering. However, we can cite here the most frequently published data of the mean longitudinal properties: Young's modulus, ultimate strength and ultimate strain, which are ~70 GPa, 700 MPa and 3%, respectively.[8] Transverse modulus is estimated to be around 8 GPa.[9]

Damage in unidirectional (UD) and cross-ply flax fibre-reinforced composites, tested under tensile loading was studied in refs [3,10,11]. At the microscopic level and at low stress, microcracks arise within the material and by growing they may lead to other forms of damage such as delamination, fibre breakage, interfacial debonding, etc. To better understand the damage phenomena and to better control the parameters which lead to failure, acoustic emission (AE) was used to monitor damage in natural fibre-reinforced composites.[10–12]

This article continues this line of research, enriching the experimental evidence and analysis of the damage processes in flax/epoxy composites in the following directions:

1. study of different laminate layups covering the typical configurations in practically used laminates;
2. combination of AE monitoring with post-mortem microscopy for identification of the damage modes;
3. special the features of damage initiation and development, which are specific to natural fibres, in contrast with man-made fibres such as glass.

Materials and test methods

The studied material is a quasi-UD woven prepreg, flax/epoxy, with areal density of the reinforcement 170 g/m^2 (95.5% flax fibres in the warp direction and 4.5% flax fibres in the weft direction), provided by LINEO (Belgium). The surface image of the prepreg is shown in Figure 2. The woven fabric is pre-impregnated with epoxy resin (prepreg system Araldite LY5150/Aradur 1571/Accelerator 1573/Hardener XB3471). The laminates were made in different configurations $[0^\circ]_8$, $[0^\circ, 90^\circ]_{2S}$, $[-45^\circ, 45^\circ]_{2S}$ and $[0^\circ, 90^\circ, +45^\circ, -45^\circ]_S$, using vacuum bag and an autoclave. The temperature and the pressure during autoclaving reached 130°C and 4 bars, respectively. The total fibre volume fraction of all the laminates is $47 \pm 2\%$.

Downloaded from jcm.sagepub.com at KU Leuven University Library on March 13, 2015

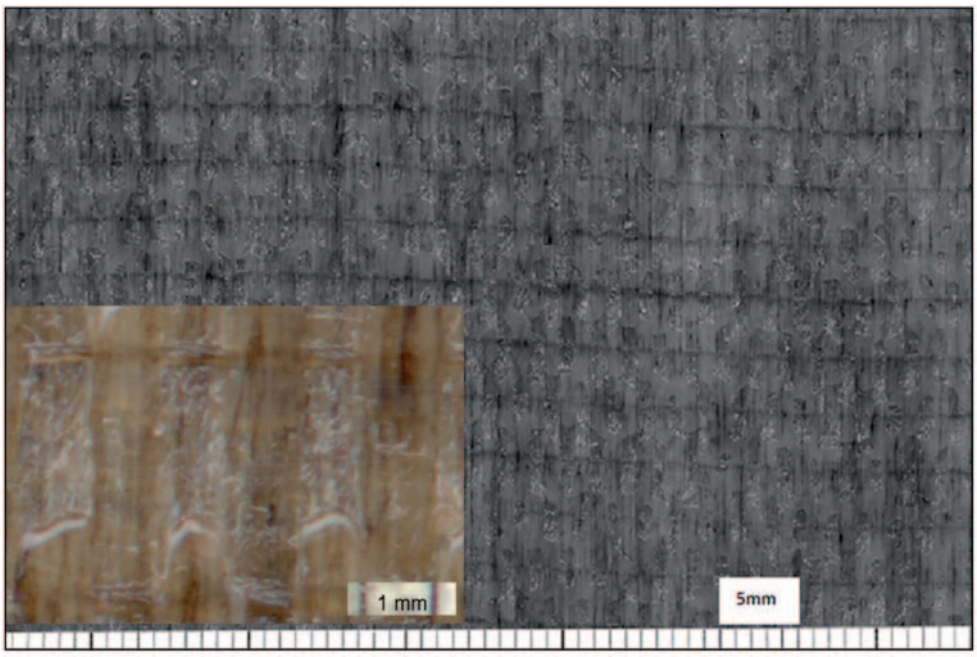

Figure 2. Surface image of the flax prepreg. Warp direction is vertical. Inset: enlarged image.

To analyse the plate cross sections, specimens of $\sim 10 \times 10$ mm were cut from the plates' edges; these cross sections, observed under an optical microscope, are shown in Figure 3. The micrographs of the laminates cross sections (Figure 3) reveal good quality of impregnation, no voids were observed in any of the prepared laminates. Rectangular samples, 250 mm long and 25 mm wide, were cut out from ~ 2 mm thick plates, using a diamond wheel saw, to be further subjected to tensile tests in the 0° direction. To avoid failure due to the stress concentration of the machine clamps, $40 \times 25 \times 5$ mm glass/epoxy composite tabs were glued at the ends of each specimen. The length of each specimen between the grips was 170 mm.

Tensile tests were performed using an INSTRON 4505 machine with a loading capacity of 100 kN and the load cell of 100 kN. The crosshead speed, temperature and humidity during the tests were 5 mm/min, 20°C and 50%, respectively. For each configuration, three tests were carried out. Stresses in the samples were calculated based on the thickness measured for each sample before the test.

To monitor in situ the damage development in the laminates, AE VALLEN equipment was used (Table 1). The traction machine was connected to the AE control unit, providing load signal. The preamplification was 34 dB, and the noise was filtered using a threshold of 40 dB. To provide a good acoustic coupling, the sensors surfaces were covered with silicon grease, and then the sensors were attached inside the gauge length approximately at the same distances from the specimen's tabs. The nominal distance between the sensors was 100 mm. AE recording was performed in another series of three tensile tests for each configuration. After identification of damage thresholds, several tests were performed with specimen loading up to certain intermediate load level. These specimens, as well as the specimens loaded till failure, were cross-sectioned and the internal structure of the laminates and damage in them was observed under optical microscope.

The strains during tensile tests were measured using a digital image correlation technique, for which a Vic2D software (the software from LIMESS Maßtechnik und Software GmbH, 2006; Table 1). The speckled black-and-white pattern on the specimen surface was made by spraying the zone of 50 mm length in the middle of the specimen. The images were taken with time interval 0.5 s. The noise in the DIC measurement was estimated based on the strain calculation for a given displacement of the specimen as rigid body and was found to be below 0.02% strain. Average strains in the direction of loading and in the transverse direction were calculated based on DIC strain maps and used for calculation of Poisson's coefficient. All strain values given in this article are DIC-average values.

Results and discussion

Stress–strain curves

Stress–strain curves for the studied laminates are presented in Figure 4. A ductile behaviour is seen for

Downloaded from jcm.sagepub.com at KU Leuven University Library on March 13, 2015

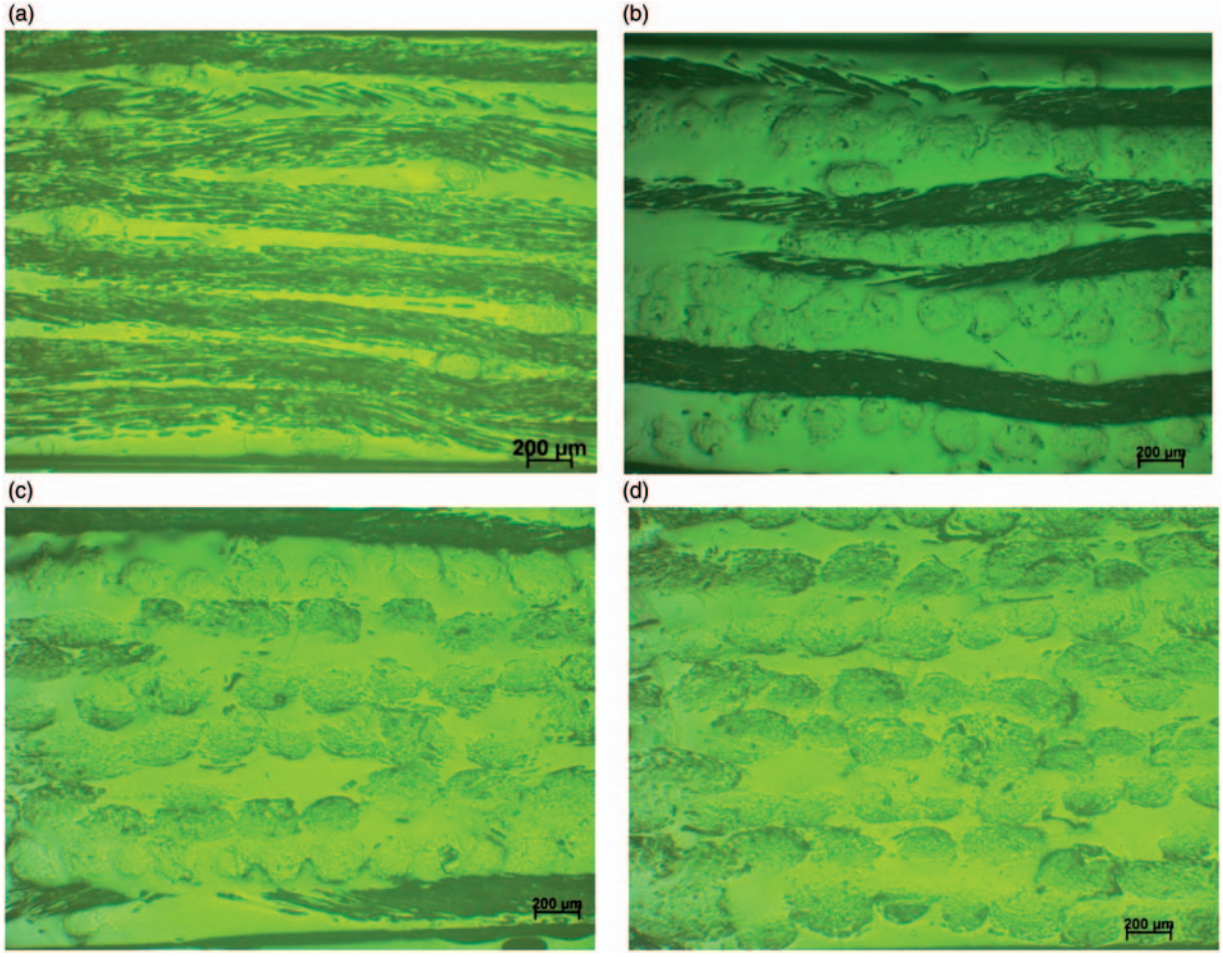

Figure 3. Cross sections of the laminates, parallel to 0° axis: (a) $[0^\circ]_8$, (b) $[0^\circ, 90^\circ]_{2S}$, (c) $[0^\circ, 90^\circ, +45^\circ, -45^\circ]_S$ and (d) $[+45^\circ, -45^\circ]_{2S}$.

Table 1. AE and strain mapping parameters.

AE parameters	
Software	AMSY-5
Amplifiers	AEP4
Amplification	34 dB
Discrimination time	400 µs
Rearm time	9.2 ms
Sample rate	5 MHz
Sensors	Resonant sensors VS375-M 100 kHz to 1 MHz
Sensor diameter	2 cm
Strain mapping	
Software	LIMESS 2Vic
Correlation subset	21 pixels
Correlation step	5 pixels
Strain window	5 pixels

$[+45^\circ, -45^\circ]_{2S}$ laminate, whereas for other laminates a brittle behaviour is observed. All the curves exhibit a non-linear behaviour at the early stage of loading. On the basis of the stress–strain measurements, the stiffness (E) during loading was evaluated, and the variation of the tangent stiffness modulus versus strain for one characteristic stress–strain diagram was plotted in the same graph. The tangent modulus value was calculated as a ratio of the stress increment to the strain increment for two subsequent readings of the stress and strain, corresponding to the strain increment of 5e-4.

Tangent modulus versus strain curves display three main parts (see labels in Figure 4a). In the first part (1), at low strains, approximately up to 0.2% of strain for the $[0^\circ]_8$, $[0^\circ, 90^\circ]_{2S}$ and $[0^\circ, 90^\circ, +45^\circ, -45^\circ]_S$ laminates and up to 0.5% of strain in the case of the $[+45^\circ, -45^\circ]_{2S}$ laminate, the curve has a plateau or somewhat constant value. This plateau defines an

Downloaded from jcm.sagepub.com at KU Leuven University Library on March 13, 2015

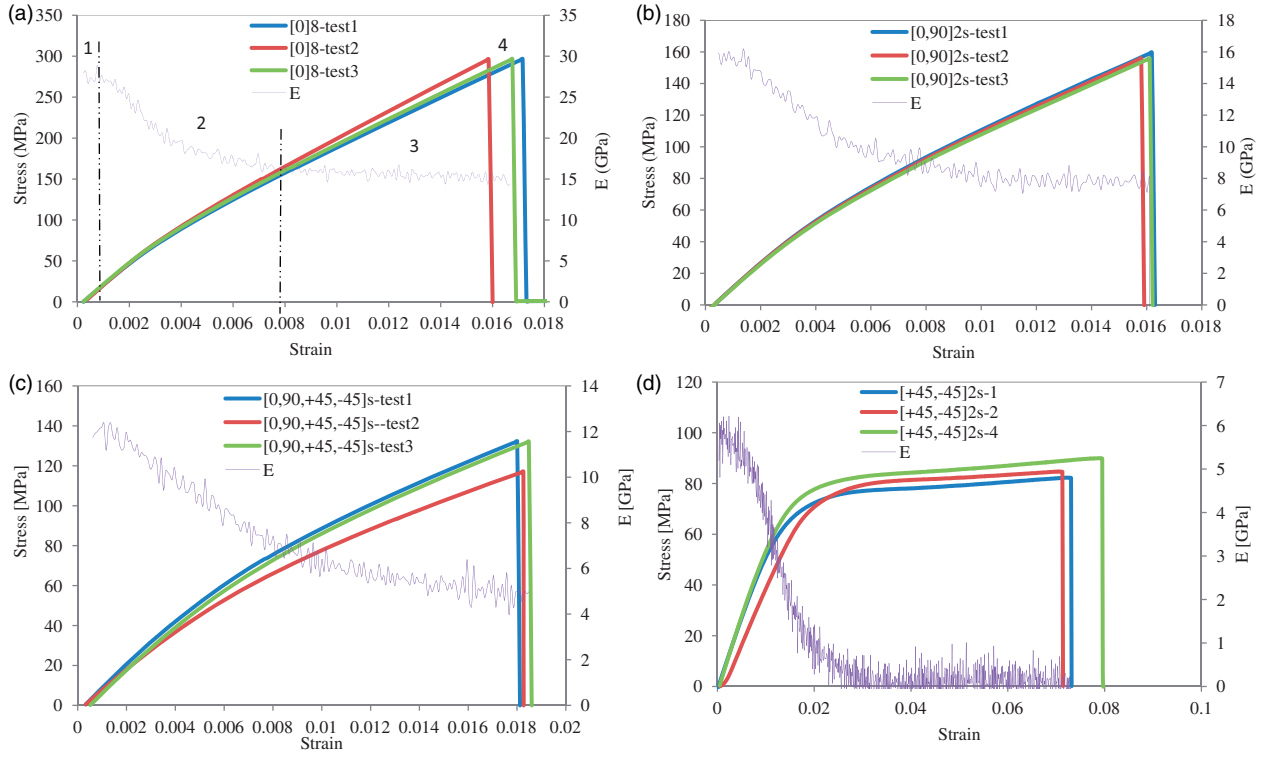

Figure 4. Stress–strain curves for all tests and stiffness–strain curve for a typical test: (a) $[0^\circ]_8$, (b) $[0^\circ, 90^\circ]_{2S}$, (c) $[0^\circ, 90^\circ, +45^\circ, -45^\circ]_S$ and (d) $[+45, -45]_{2S}$.

Table 2. Summary of tensile tests and AE results.

	Tensile tests results					AE results	
Laminate	Linearity threshold strain (%)	Initial Young's modulus (GPa)/estimated value (see text)	Poisson's ratio	Ultimate strength (MPa)	Ultimate strain (%)	Damage threshold, strain (%)	Maximum AE energy (a.u.)
$[0^\circ]_8$	0.12	$27.2 \pm 0.52/33.1$	0.409 ± 0.034	296 ± 0.5	1.65 ± 0.055	0.45	5.86×10^7
$[0^\circ, 90^\circ]_{2S}$	0.14	$15.7 \pm 0.15/18.1$	0.126 ± 0.014	158 ± 2	1.62 ± 0.5	0.54	2.35×10^6
$[0^\circ, 90^\circ, +45^\circ, 45^\circ]_S$	0.20	$11.9 \pm 0.6/13.5$	0.319 ± 0.259	126 ± 7.5	1.76 ± 0.15	0.8	1.8×10^5
$[+45^\circ, -45^\circ]_{2S}$	0.5	$5.7 \pm 0.11/9.0$	0.566 ± 0.064	85 ± 4	7.47 ± 0.415	0.87	2.9×10^4

Note: The scatter gives the standard deviation in three tests.

interval of linearity of the stress–strain curve, the maximum strain in this interval will be called 'linearity threshold strain' (see Table 2). This plateau is followed by a second part (2) where the curve decreases rapidly and continuously, terminating by the region (3) where the modulus decreases much slowly until the failure of the laminate (4). The Young's modulus for the different composites was then calculated by averaging the modulus values in the linearity interval, up to the linearity threshold given in Table 2. Young's modulus values and the main mechanical properties: ultimate strength, ultimate strain and Poisson ratio, identified from stress–strain curves and DIC measurements are listed in Table 2.

It is instructive to compare the measured Young's moduli with the values, which can be obtained using micromechanical homogenisation of the plies and Classical Laminate Theory (CLT) under assumption of ideal UD structure of the plies. The calculations using Chamis formulae for homogenisation (fibre longitudinal (L) and transverse (T) moduli $E_L = 70$ GPa and $E_L = 8$ GPa, Poisson's coefficient $\nu_{LT} = \nu_{TT} = 0.25$,

Downloaded from jcm.sagepub.com at KU Leuven University Library on March 13, 2015

Young's modulus of the matrix 2.7 GPa, Poisson's coefficient 0.4, fibre volume fraction 47%) and CLT formulae give the values for the laminates, which are shown in Table 2. The measured values are systematically below the estimations, which are explained by the crimp of the yarns and curvature of the fibres inside them, caused by their twist (ca. 100 turns/m). The crimp, caused by the presence of weft yarns (albeit well-spaced), is evident in the micrographs of the laminate cross section (Figure 3a). The angle of the warp yarn inclination in relation to the middle surface of a woven ply can be estimated as lying in the range from few degrees for the most part of the yarn up to $15 \ldots 20^\circ$ near the intersection with a weft yarn.

One can observe a slight difference in the onset of non-linearity between the $[0^\circ]_8$ and $[0^\circ, 90^\circ]_{2S}$ laminates, which happens at ~0.12% and 0.14% of strain, respectively. In the laminates with 45° layers the non-linearity occurs at a higher strain value being 0.2% of strain in $[0^\circ, 90^\circ, +45^\circ, -45^\circ]_S$ and 0.5% of strain in $[+45^\circ, -45^\circ]_{2S}$ laminate. This is explained by the fact that strain in the direction of the fibres in 45° plies is lower than the strain applied at 0° direction, and we will see below that the non-linearity is a consequence of the intrinsic non-linearity of flax fibres, hence is controlled by the strain in the direction of fibres in the laminate plies.

The non-linearity of the stress–strain curves of the flax laminates when loaded in the fibre direction has the same character as the intrinsic non-linearity of flax fibres, observed in refs [6,7] and discussed in the 'Introduction' section earlier. The same behaviour was also reported in ref. [11] for UD flax fibre composites. The two main stages of tangent modulus evolution, an initial constant value followed by a decrease at $0.1 \ldots 0.3\%$ strain, was found in both studies, to be followed at higher strains by a new increase in stiffness, with the final linear section of the curve.[7] This behaviour is very close to the one observed in our measurements for the initial part of the stress–strain curve.

Apart from the similarities, there are differences in behaviour of single flax fibre or UD flax/polyester composites, reported in refs [7] and [11], respectively, and quasi-UD woven flax/epoxy laminates studied in this work. To highlight the difference between these cases, the normalised stress–strain curves for a single flax fibre[7] and the studied flax/epoxy composite were plotted in the same graph – Figure 5. Single fibres, and 'ideal' UD flax composites exhibit a change of the stiffness after linearity threshold: first significant decrease of the stiffness, then its increase to values close to the initial modulus. In the case of quasi-UD laminate, the stiffness decreases monotonically after the linearity threshold to reach a constant value about ½ of the initial modulus (Figure 4a). The difference can be explained by the fact that in the quasi-UD woven fabric considerable crimp of the yarns/fibres increases the local strain in the fibres, and the fact that the flax yarns are slightly twisted. The crimp leads to difference of the strain in different yarns and in different section of the yarns. The intrinsic variations of the fibre stiffness happen on different corresponding moments of the specimen deformation and are reflected in the measured specimen's stress–strain curve collectively, in certain averaged manner. This leads to a change of the stiffness

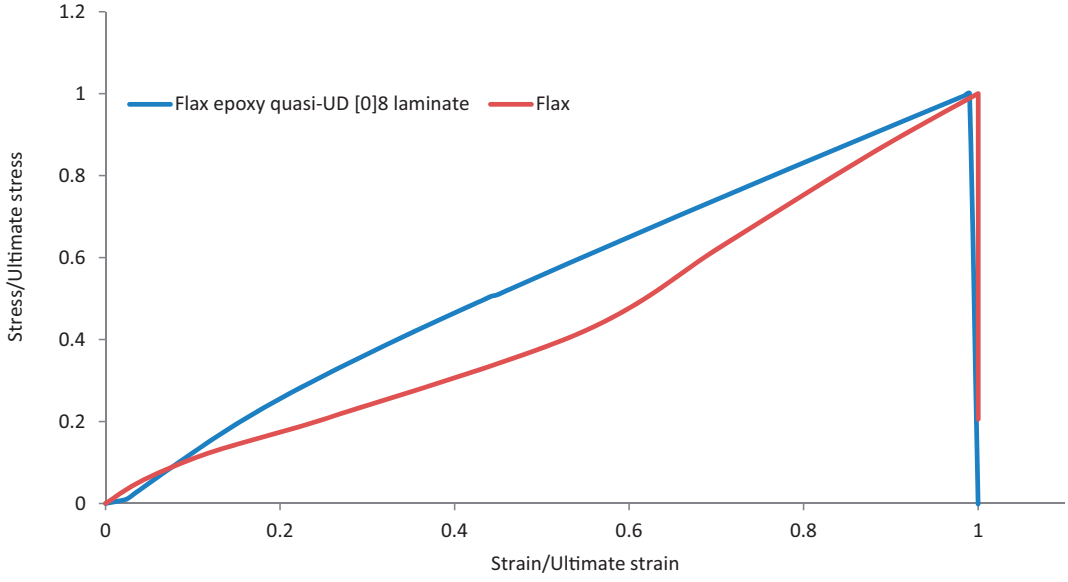

Figure 5. Normalised stress–strain curves in a single flax fibre (after[7]) and in the studied flax/epoxy $[0^\circ]_8$ laminate.

Downloaded from jcm.sagepub.com at KU Leuven University Library on March 13, 2015

variation trend to the observed monotonic decrease. Finally, the stiffness continues decreasing, but with much slower rate. However, it does not stabilise as it does for individual fibres.

In the $[0°, 90°]_{2S}$ laminate the curve (Figure 4b) shows the behaviour which is practically the same as for $[0°]_8$ laminate, which means that the non-linearity of the cross-ply laminate is mainly caused by the intrinsic non-linearity of the fibres in the 0° layers. The stress values, in comparison with the ones for $[0°]_8$ laminate, are consistent with the fact that now ½ of the fibres is oriented transversely and does not contribute significantly to the average stress. The trend of the stiffness change is quite similar to the one common for cross-ply or woven glass composites,[13,14] but is caused by different mechanisms. In glass composites, the intrinsic stiffness of fibres does not change with strain. The loss of stiffness of the cross-ply laminate is caused by cracks in 90° plies or yarns, which reduce the input of these plies/yarns in the total stiffness. We will see in 'Microscopy observations' section that in the studied cross-ply flax composite transverse cracks appear late, just before the final failure of the specimen. There is no contribution of transverse cracking to the composite stiffness decrease, which is caused fully by intrinsic change of the fibre stiffness. An interesting analogy for this phenomenon is relation between the intrinsic stiffness increase of carbon fibres and stiffness change during tensile loading of textile carbon-reinforced composites.[15,16]

With the presence of bias (±45°) plies in the laminate an additional factor starts playing a role: non-linear plastic behaviour of the matrix, which manifests itself ultimately in quasi-ductile behaviour of $[+45, -45]_{2S}$ laminates (Figure 4d) with a wide non-linear region of the tensile diagram and low final stiffness, defined by the possible fibre rotation – the behaviour common for bias loading of cross-ply laminate with glass or carbon fibres as well.[17,18] Stress–strain diagram of the quasi-isotropic laminate $[0°, 90°, +45°, -45°]_S$ is generally similar to [0°,90°], with the difference of more smooth change of stiffness and continuing stiffness decrease up to failure of the sample – features which can be explained by combination of almost bilinear diagram of $[0°, 90°]$ and fast and deep stiffness decrease of $[+45°, -45°]$.

Acoustic emission results

The damage initiation and development in the studied laminates were monitored using AE. The AE activity recorded during tensile tests is reported in terms of energy and number of AE events. Figure 6 shows

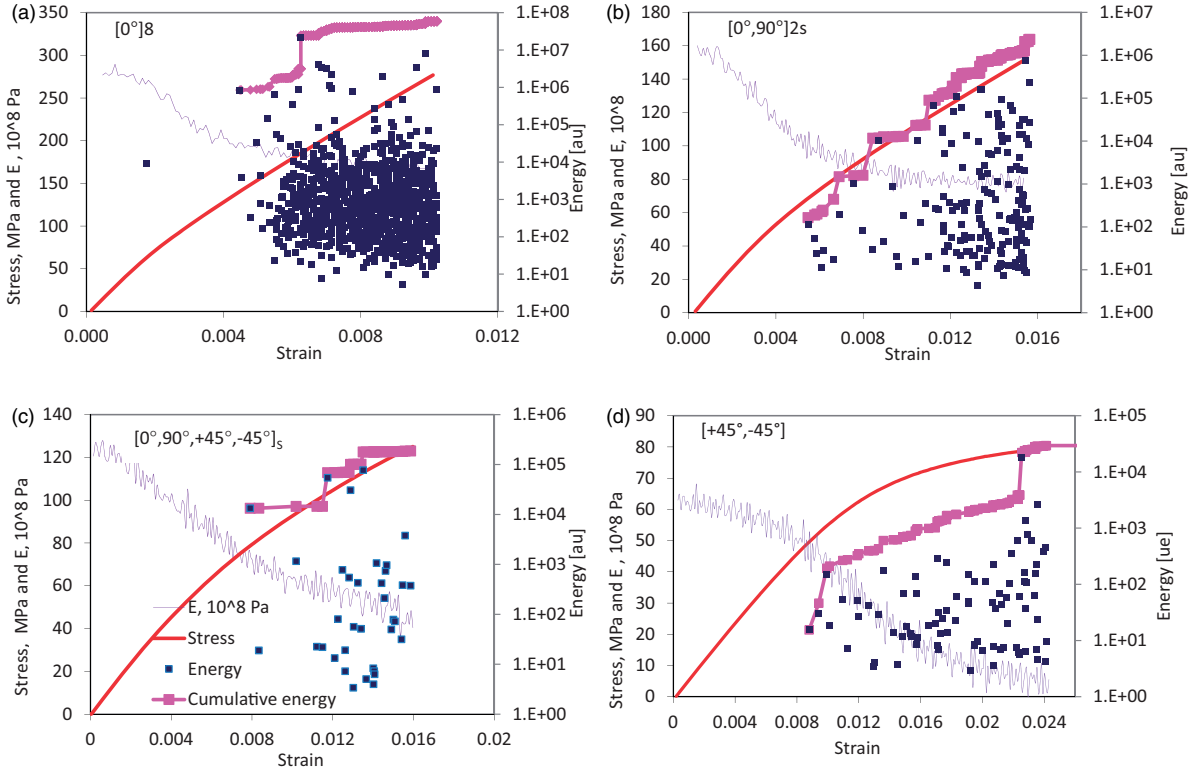

Figure 6. AE events energy, cumulative AE energy, stress and stiffness versus strain, a typical test: (a) $[0°]_8$, (b) $[0°, 90°]_{2S}$, (c) $[0°, 90°, +45°, -45°]_S$ and (d) $[+45°, -45°]_{2S}$.

Downloaded from jcm.sagepub.com at KU Leuven University Library on March 13, 2015

events AE energy versus strain, cumulative energy versus strain, stress–strain and stiffness–strain dependencies in the same graph. To avoid their damage, AE sensors were removed before the final failure of the specimen, at ~65...80% of the final failure stress (e.g. at 1% strain for 0° laminates, whereas the real failure strain is 1.6%).

The analysis of the AE diagrams allowed us to identify the damage thresholds in the different laminates. It is apparent that the threshold of damage is the lowest in the $[0°]_8$ laminate being 0.45% strain. The AE diagram for $[+45°, -45°]_{2S}$ (Figure 6d) shows the highest damage initiation value, which reaches ~0.87% strain. The damage threshold strains (average for three tests) are shown in Table 2 for all the studied laminates. The damage thresholds definition is based not on absolute value of the AE energy, but on the change in the cumulative AE energy curve shape. However, the use of certain threshold for AE noise filtering (40 dB) relies on low attenuation of the signal on few centimetres length, and no loss of information due to this filtering. As discussed below, the signals below the noise filter level may be caused also by damage events on the microstructural level of the fibres.[11]

The remarkable feature of the AE activity is the fact that the damage threshold strain is at least two times higher than the linearity threshold. This highlights the observation made earlier, that the observed stress–strain non-linearity is caused by the intrinsic change of stiffness of flax fibres, even in absence of damage in the laminate – which is shown by the absence of AE events.

The AE characteristics in $[0°]_8$ laminate, registered in our tests, correspond to observations made in ref. [11]. With the test configuration and specimens dimension close in our work and in ref. [11], one can cautiously assume that the AE event amplitudes in these tests can be considered similar one to another. For UD flax/polyester composites, tested in that work, AE activity with amplitude in the range 20...40 dB starts at strain of 0.9%, well above the linearity threshold. The lower amplitude events, observed in ref. [11] to start together with onset of non-linearity (yield point), are explained in ref. [11] as being connected to microstructural failure events within elementary fibres – or, in other words, with intrinsic change of the fibre stiffness. Our measurements confirm this conclusion in ref. [11] not only for UD laminates but also for more complex flax fibre reinforcement architectures: quasi-UD laminates with yarn crimp, cross-ply and quasi-isotropic laminates. For all these materials, as evidenced by the curves in Figure 6(a) to (c) and data in Table 2, the onset of AE activity happens much later than the stress–strain curve becomes non-linear.

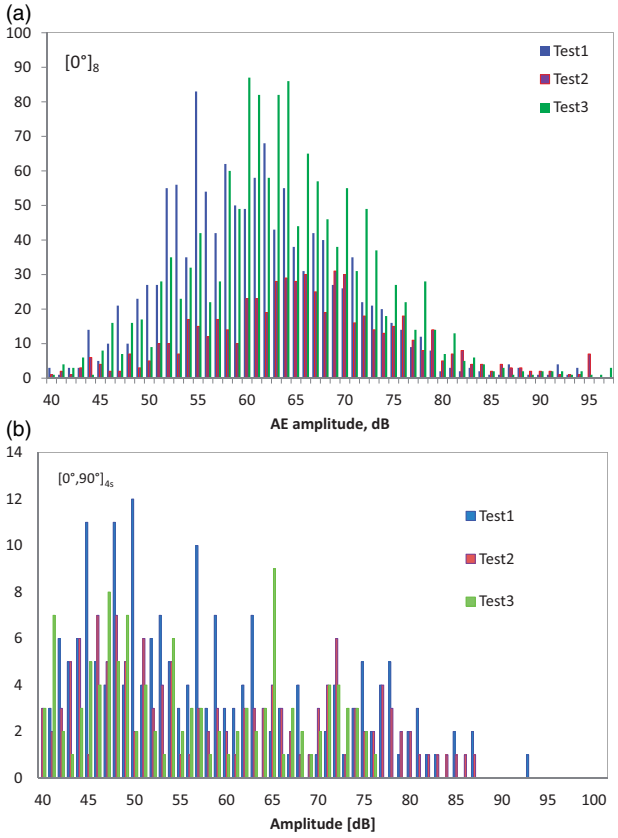

Figure 7. Distribution of AE events amplitude in $[0°]_8$ (a) and $[0°, 90°]_{4S}$ (b) laminates, three tests.

For $[+45°, -45°]_S$ laminate AE threshold is also later than onset of non-linearity of stress–strain curve. However in this case of off-axis, bias loading this phenomenon is quite common also for glass-reinforced laminates,[13,18] with no intrinsic change of the fibre stiffness, and explained mainly by plastic behaviour of the matrix. Further discussion in this section will be focused on $[0°]_8$, $[0°, 90°]_{2S}$ and $[0°, 90°, +45°, -45°]_S$ laminates, which demonstrate pecularities of flax fibre behaviour.

Once started, damage in composites, presumably causing the observed AE activity, contributes to the decrease of stiffness. Instead of the constant stiffness of flax fibres at high strains, the laminates demonstrate stiffness decrease, albeit slow, for high strain region as well. The difference from the 'constant stiffness at high strain' behaviour of individual fibres can be explained by on-going damage in the matrix or fibre/yarns – matrix interface (see 'Results and discussion' and 'Conclusion' sections below).

Comparison of the AE events registration in Figure 6, sections a–c, for $[0°]_8$, $[0°, 90°]_{2S}$ and $[0°, 90°, +45°, -45°]_S$ laminates suggests that the

Downloaded from jcm.sagepub.com at KU Leuven University Library on March 13, 2015

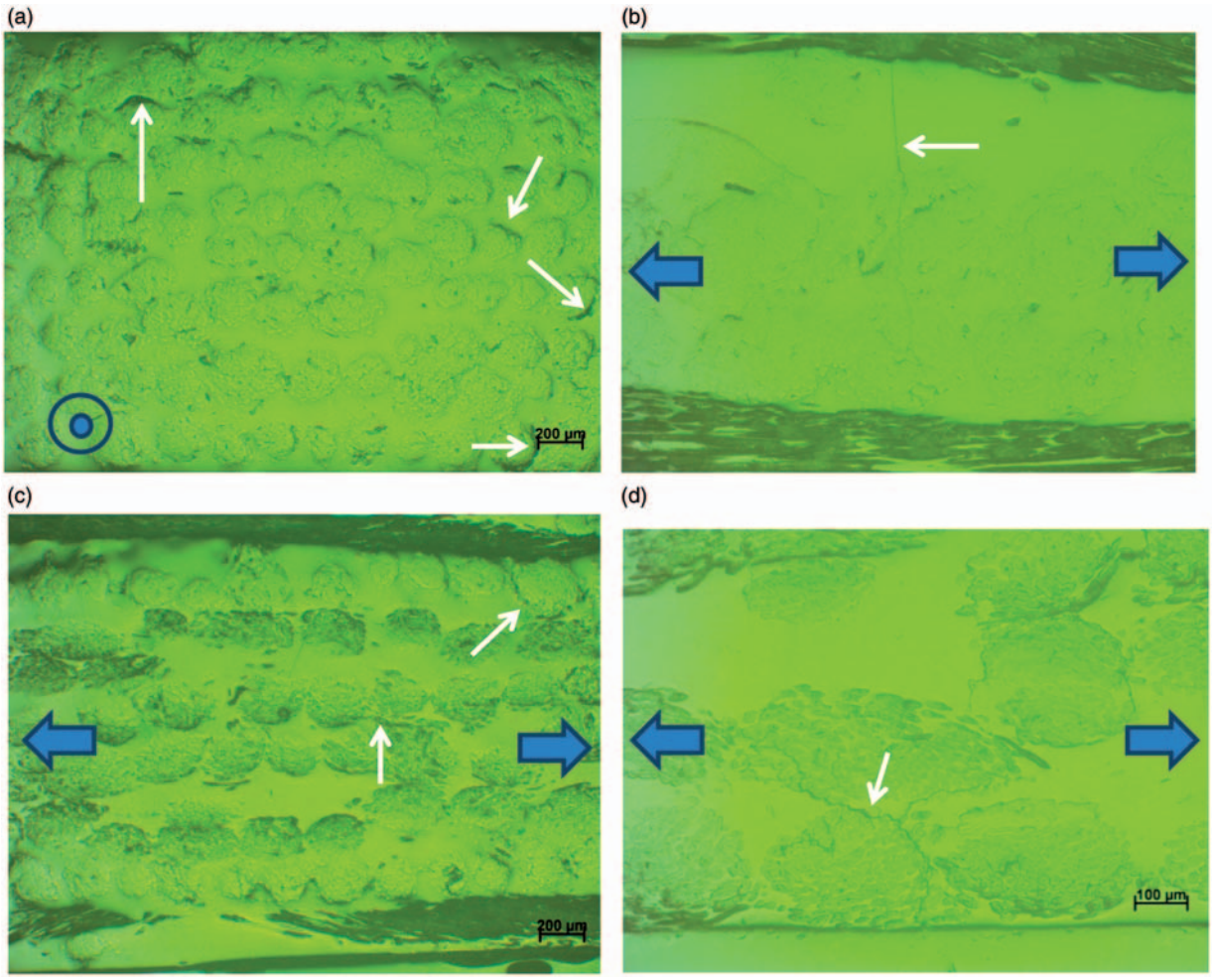

Figure 8. Micrographs of the failed samples, cross sections made in the proximity to the fracture region: (a) $[0^\circ]_8$ laminate, section normal to the loading direction, arrows show longitudinal cracks on yarn/matrix interface; (b) $[0^\circ, 90^\circ]_{4S}$ laminate, section in the direction of loading, arrows show a transversal crack; (c) $[0^\circ, 90^\circ, +45^\circ, -45^\circ]_S$ laminate, section in the direction of loading, arrows show cracks on yarn/matrix interface and (d) $[+45^\circ, -45^\circ]_{2S}$ laminate, section in the direction of loading, arrows show cracks on yarn/matrix interface.

number of the registered events is strongly linked to the amount of 0° fibres. This allows hypothesising that the AE events are mainly linked to fibre damage and damage associated with 0° fibres and yarns – a hypothesis supported by the fact that matrix fracture is observed only at late stages of loading (see 'Results and discussion' and 'Conclusion' sections below). Figure 7 analyses further the distribution of AE events amplitude for UD and cross-ply laminates. For the former (UD, Figure 7a), the distribution has a roughly Gaussian shape with an average peak value around 60 dB. This value of amplitude is close to the one (55 dB) ascribed to the fibre breakage.[10,12] In cross-ply laminate (Figure 7b), the distribution is more uniform, suggesting that damage (matrix? interface?) leads to appearance of AE events with lower and higher amplitudes.

Microscopy observations

The AE analysis was further supported by optical observations, as illustrated in Figure 8. The specimens loaded till failure and till intermediate stages of loading were cross-sectioned and the polished cross sections studied under an optical microscope. Cracks on interface of the yarns and technical fibres were observed in specimens starting from the applied strain level corresponding to onset of the AE activity. Presumably weak adhesion of epoxy resin to flax fibres can be a reason for early occurrence of these cracks. The appearance of these cracks is the same for different stages of loading, hence only the failed specimens are shown in Figure 8, as they reveal most clearly the damage features. These interface cracks appear in longitudinal, transverse and shear loading of the plies. The cracks on interface of

Downloaded from jcm.sagepub.com at KU Leuven University Library on March 13, 2015

individual technical fibres and yarns do not coalesce into longer cracks, but can form a 'cluster' of cracks in neighbouring yarns.

Contrary to expectations, transverse cracks in 90° and ±45° plies were not found till the final stage of the loading. This behaviour is very different to what is observed in glass fibre-reinforced laminates. This can be attributed to the low stress concentrations in transverse direction due to the low transverse modulus of flax fibres (ca. 8 GPa). One can also argue that the damage in flax laminates follows the weakest place, namely fibre-matrix debonding (because of the low adhesion), while in glass fibre laminates with stronger interface between fibres and matrix transverse cracks in the matrix are the prevailing damage mechanism, caused by stress concentrations due to high stiffness contrast between fibres and matrix.

The related feature, also different from what is seen in glass-reinforced composites, is morphology of longitudinal cracks on interface of the yarns (these cracks can be called 'debondings' or 'splitting'). In glass fibre-reinforced composites, these local debondings are normally a result of interaction of a transverse crack with an interface. Hence, the 'debonding' cracks are normally parallel to the lamina plane. In flax quasi-UD woven composites, as it can be seen in Figure 8(a), the longitudinal debondings of yarns interface can be positioned on any side of the yarn. These debondings should be linked to intra-yarn and intra-fibres cracks, as suggested in ref. [11].

Conclusion

In this study, the mechanical properties and damage behaviour of flax/epoxy quasi-UD woven $[0°]_8$, $[0°, 90°]_{2S}$, $[0°, 90°, +45°, -45°]_S$ and $[+45°, -45°]_{2S}$ laminates were investigated. The main findings can be summarised as follows:

1. The stress–strain curves show that the $[+45°, -45°]_{2S}$ laminates exhibit ductile behaviour, while $[0°]_8$, $[0°, 90°]_{2S}$, $[0°, 90°, +45°, -45°]_S$ and $[+45°, -45°]_{2S}$ are rather brittle. The stress–strain curves exhibit a specific bilinearity, which is attributed to the intrinsic change of stiffness of flax fibres with deformation. The linearity threshold is in the range of 0.12…0.2% strain for $[0°]_8$, $[0°, 90°]_{2S}$, $[0°, 90°, +45°, -45°]_S$ laminates and 0.5% strain for $[+45°, -45°]_{2S}$.
2. Damage initiation thresholds, determined using AE, are found to be 0.45% strain for $[0°]_8$ laminate, 0.54% strain for $[0°, 90°]_{2S}$, 0.8% strain for $[0°, 90°, +45°, -45°]_S$ and 0.85% strain for $[+45°, -45°]_{2S}$. The damage thresholds are much higher than the linearity threshold. The damage thresholds for $[0°, 90°]_{2S}$ and $[0°, 90°, +45°, -45°]_S$ are considerably higher than the damage thresholds typically observed in glass fibre woven cross-ply and quasi-isotropic laminates.
3. The damage mechanisms in quasi-UD woven flax fibre laminates are governed by damage processes in elementary flax fibres, which are transferred to the inter-fibre, inter-yarn and inter-ply meso-scale level in the form of technical fibres or yarn debondings, localised in the scale of a yarn diameter. Matrix cracks through plies are formed in 90° plies only at very late stages of loading, prior to failure of the specimen and are not found in 45° plies.

The observed absence of transverse cracking in flax-reinforced composites may open new perspectives in exploiting the advantages of natural fibre composites. In particular, observations in refs [19,20] suggest a direct link between the damage thresholds in quasi-static loading and the fatigue limit in glass- and carbon-reinforced composites. Investigation of this link for natural fibre composites may open new perspectives for damage-driven applications of 'green' materials.

Acknowledgements

The authors are grateful to the laboratory staff of the Department MTM: Manuel Adams, Paul Crabbe, Kris Van de Staey and Johan Vanhulst – for their help needed to successfully perform the experiments presented in this work, and to Dr K. Charlet (UCL), who has kindly provided us the raw data of the experiments described in ref. [7] for use in Figure 5.

Conflict of interest

None declared.

Funding

The research visit of Malika Kersani to KU Leuven was funded by the Ministry of Higher Education and Research of Algeria (grant number FWOG.035409) and supported by Department MTM, KU Leuven in the scope of a BioBuild project, funded by the Seventh Framework Program of European Commission (grant number 285689).

References

1. Muralidhar BA, Giridev VR and Raghunathan K. Flexural and impact properties of flax woven, knitted and sequentially stacked knitted/woven preform reinforced epoxy composites. *J Reinforc Plast Compos* 2012; 31: 379–388.
2. Slattery ATI. Some observations on the size and shape of the flax fibre ultimates. *J Text Inst Trans* 1936; 27: T101–T108.

Downloaded from jcm.sagepub.com at KU Leuven University Library on March 13, 2015

3. Rask M, Madsen B, Sørensen BF, et al. In situ observations of microscale damage evolution in unidirectional natural fibre composites. *Compos Part A* 2012; 43: 1639–1649.
4. Morvan C, Andème-Onzighi C, Girault R, et al. Building flax fibres: more than one brick in the walls. *Plant Physiol Biochem* 2003; 41: 935–944.
5. Bos HL, Müssig J and van den Oever MJA. Mechanical properties of short-flax-fibre reinforced compounds. *Compos Part A* 2006; 37: 1591–1604.
6. Baley C. Analysis of the flax fibres tensile behaviour and analysis of the tensile stiffness increase. *Compos Part A* 2002; 33: 939–948.
7. Charlet K, Eve S, Jernot JP, et al. Tensile deformation of a flax fiber. *Procedia Eng* 2009; 1: 233–236.
8. CELC. *Flax and Hemp fibres: a natural solution for the composite industry*. Paris: JEC Composites, 2012.
9. Barley C, Perrot Y, Busnel F, et al. Transverse tensile behaviour of unidirectional plies reinforced with flax fibres. *Mater Lett* 2006; 60: 2984–2987.
10. Romhány G, Karger-Kocsis J and Czigany T. Tensile fracture and failure behavior of thermoplastic starch with unidirectional and cross-ply flax fiber reinforcements. *Macromol Mater Eng* 2003; 288: 699–707.
11. Hughes M, Carpenter J and Hill C. Deformation and fracture behaviour of flax fibre reinforced thermosetting polymer matrix composites. *J Mater Sci* 2007; 42: 2499–2511.
12. De Rosa IM, Santulli C and Sarasini F. Acoustic emission for monitoring the mechanical behaviour of natural fibre composites: a literature review. *Compos Part A* 2009; 40: 1456–1459.
13. Lomov SV, Bogdanovich AE, Ivanov DS, et al. A comparative study of tensile properties of non-crimp 3D orthogonal weave and multi-layer plain weave E-glass composites. Part 1: materials, methods and principal results. *Compos Part A* 2009; 40: 1134–1143.
14. Ivanov DS, Lomov SV, Bogdanovich AE, et al. A comparative study of tensile properties of non-crimp 3D orthogonal weave and multi-layer plain weave E-glass composites. Part 2: Comprehensive experimental results. *Compos Part A* 2009; 40: 1144–1157.
15. Bogdanovich AE and Lomov SV. Non-hookean behavior of carbon fiber textile composites. In: *Proceedings of the 11th International Conference on Textile Composites (TexComp-11)*, Leuven, 2013. electronic edition, s.p.
16. Bogdanovich AE, Karahan M, Lomov SV, et al. Quasi-static tensile behavior and progressive damage in carbon/epoxy composite reinforced with 3D non-crimp orthogonal woven fabric. *Mech Mater* 2013; 62: 14–31.
17. Wisnom M. The effect of fibre rotation in $+-45^{\circ}$ tension tests on measured shear properties. *Compos Part A* 1995; 26: 25–32.
18. Naik GN and Ganeshi VK. (± 45) Degree off-axis tension test for shear characterization of plain weave fabric composites. *J Compos Technol Res* 1997; 19: 1–9.
19. Lomov SV, Carvelli V and Verpoest I. Correlations between damage initiation thresholds in textile composites and fatigue life limits. In: *Proceedings of the 10th International Conference on Textile Composites (TexComp-10)* (eds C Binetruy and F Boussu), 2010, pp. 475–481.
20. Lomov SV, Gorbatikh L, Verpoest I, et al. Damage initiation thresholds in textile composites and fatigue life limits In: *Proceedings of the 6th. Technical Conference of SAMPE Europe (SETEC-11)*, Leiden, 2011, pp. 59–66.

Downloaded from jcm.sagepub.com at KU Leuven University Library on March 13, 2015